Excimer Formation by Electric Field Induction and Side Chain Motion Assistance in Polyfluorenes

Hsin-Hung Lu, Ching-Yang Liu, Tzu-Hao Jen, Jin-Long Liao, Hao-En Tseng, Chih-Wei Huang, Ming-Chin Hung, and Show-An Chen*

Department of Chemical Engineering, National Tsing-Hua University, Hsinchu, 30013 Taiwan, R.O.C.

Received July 21, 2005; Revised Manuscript Received September 19, 2005

ABSTRACT: For poly(9,9-di(6-(2-(3-oxetanyl)butoxyl)hexyl)-2,7-fluorene) (POBOHF), measurements on field induction−thermally stimulated current (FI-TSC) and electroluminescence (EL) under a wide temperature range demonstrate that electric field induction (FI) accompanied by side chain motion can lead to a formation of excimers, which contribute to a growth of a green component in the EL spectrum. This phenomenon also happens to poly(9,9-di-*n*-octyl-2,7-fluorene) (PFO), especially under long-term operations with higher electric fields (1×10^6 V/cm), copolymers of OBOHF and FO (PF-1/1 and PF-1/3), and even cross-linked POBOHF. The higher polarity of the side chain in the polyfluorenes (PFs) can cause a more pronounced FI effect. For POBOHF, the green component can even dominate after a few cycles of device operation. Lowering the content of cross-linkable commoner in the copolymers from 50 to 25 mol % only moderately suppresses the formation of FI excimers.

Introduction

The applications of conjugated polymers in light-emitting diodes,[1,2] field-effect transistors,[3,4] and plastic solar cells[5,6] have attracted great attention recently. In polymer light-emitting diodes (PLED), polyfluorenes (PFs) are promising candidates as blue emitters due to their high photoluminescence quantum efficiencies (PLQEs) as solid films, for example, as high as 59% for as spin-coated poly(9,9-di-*n*-octyl-2,7-fluorene) (PFO),[7] excellent solubility and film-forming ability, and ease in controlling their properties via facile substitution in the 9,9-position of the fluorene unit.[8−11] However, it was found to be difficult for PFs to obtain pure and stable blue light emission due to a presence of undesirable green emission from the electroluminescence (EL) device.[12−15] Two explanations have been given for the green emission: one was the keto defect,[16−20] and the other was excimer or aggregate emission.[12,16,21−24]

Excimer is a delocalized and lower energy excited-state complex, which is generated by an interaction of an excited chromophore with a ground-state chromophore,[16,25,26] and appears not only in aromatic molecules but also in polymer systems. Conwell et al.[27] found that cyano-substituted poly(*p*-phenylenevinylene) (CN-PPV) exhibited excimer emission due to its small inter-segmented distance (3.4 Å) resulting from the high electron affinity of cyano group. Excimer emission was also found to appear in poly(2,5-di-*n*-octyloxy-1,4-phenylenevinylene) (DO-PPV) after thermal treatment.[28] In PFs, excimers or aggregates could form by interchain interactions due to its stiff and planar chain geometry[26] and by interactions either between polar end groups[29] or due to the appearance of oligomers.[30] And several reports suggested methods to reduce this poor spectral purity, such as introduction of other chromophores into main[21] or side[31−33] chains, cross-linking in film states via styryl end groups,[34] end-capping,[13,29] removal of low molecular weight parts,[30] and blending with a polymer possessing higher glass transition temperatures.[35] However, some of these reports only showed EL spectra measured at certain applied voltages but did not reveal whether the emission color would still remain after a cyclic operation.

Many studies pointed out that the keto defect in PFs could cause an undesired green emission,[36−39] which might originate from an oxidation of 9-monoalkylated fluorenes during polymerization,[17,40] after photooxidation[16,17] or thermal oxidation[18−20] in air, during thermal deposition of calcium as cathode[36] (according to Gamerith et al.,[41] the defect so generated is spatially located close to the cathode and is different from the "well-described keto-type bulk defect"), and from operation of a device, especially under atmospheric conditions.[17] However, no direct evidence such as infrared data was provided to support the occurrence of keto defect for the latter two situations. On the other hand, since heat[42] and applied electric field[43] may alter morphology of polymer films and thus their emission properties, an investigation on their effects resulting from cyclic device operations is necessary.

Here we investigate reasons that cause variations in the EL spectrum during continuous operations of PFs-based devices and find that local segmental alignment of main chains induced by applied electric field under relaxation of side chains can induce the formation of excimers, which contribute to the green component of the emission. Moreover, the extent of excimer formation increases with content of polar side chains, and the FI excimer formation is hard to suppress even after cross-linking. The structures of the PFs investigated are given in Chart 1.

Experimental Section

Syntheses of Monomers and Polymers. Syntheses of the monomers and polymers used in this article are described in detail in the Supporting Information (SI).

Instrumentation. Gel permeation chromatography (GPC), device fabrication, spectroscopic measurements (including ultraviolet−visible (UV), photoluminescence (PL), photo-

* Corresponding author. E-mail: sachen@che.nthu.edu.tw.

10.1021/ma051594z CCC: $30.25 © 2005 American Chemical Society
Published on Web 11/24/2005

Chart 1. Chemical Structures of Homopolymers and Copolymers Studied in This Article

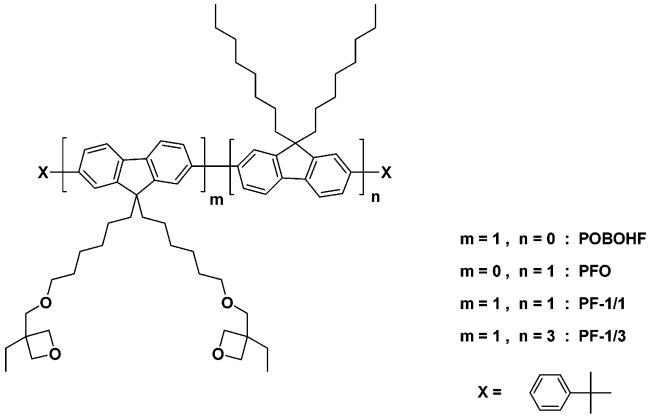

luminescence excitation (PLE), electroluminescence (EL), and Fourier transform infrared (FTIR)), field induction−thermally stimulated current (FI-TSC) measurement, and cross-linking procedure for POBOHF are also described in detail in the SI.

Results and Discussion

1. Characterization of Green Component in the Emissions from POBOHF- and PFO-Based Devices. Figure 1 shows EL spectra at room temperature measured at different applied voltages for the same POBOHF-based device. We collected EL spectra successively at 5, 7, and 10 V, and for the subsequent six spectra, all at 8 V was applied for every 20 s interval before taking the spectrum. It is obvious that the emission spectrum of POBOHF changes during the device operation and even at the first cycle is different from its corresponding photoluminescence (PL) spectrum (the inset of Figure 1), in which three vibronic emission peaks appear at 426, 446, and 476 nm. For the first cycle at 5 V, the EL shows broad emission band peaked at 424, 452, and 485 nm as well as two shoulders at 520 and 570 nm. The blue component (400−460 nm) decreases consecutively while operating at 7 and 10 V for the second and third cycles, respectively. The green component (460−650 nm) dominates the EL spectra since the second cycle, and only the green component remains after the sixth cycle. Similar variation of EL emission with applied voltages also happens to PFO as shown in Figure 2. For the first cycle at 8 V, the blue emission peaked at 424 and 446 nm as well as a green component ranging from 460 to 650 nm with two peaks at 480 and 520 nm appearing, which is different from its corresponding PL spectrum (the inset of Figure 2) characteristic of three vibronic emissions at 423, 444, and 475 nm. Under the high electric fields (($0.8-1.2$) $\times$ 10^6 V/cm), the green component grows gradually accompanied by the cyclic operations, and its intensity exceeds that of the blue component at the sixth cycle. In this article, applying high electric fields to PFO-based device is for investigation of effects of electric field on the EL emission, and such high fields can really occur in long-term operation of the device since increasing applied voltage has to be maintained to compensate for a decay in device efficiency. As can be seen, the extent of green emission of PFO is much lower than that of POBOHF. (The reason for the occurrence of this phenomenon will be revealed in section 4.) We must emphasize that, for PFO-based device whose PFO film is spin-coated from its tetrahydrofuran solution, the extent of green emission is relatively smaller, especially under cyclic operations with lower applied field (0.7×10^6 V/cm); the EL spectrum remains almost unchanged and resembles the PL spectrum in the inset of Figure 2 (relative EL intensity heights at 422, 448, and 480 nm are 1:0.60:0.43, and a long-wavelength tail (500−650 nm) also appears with very lower intensity).

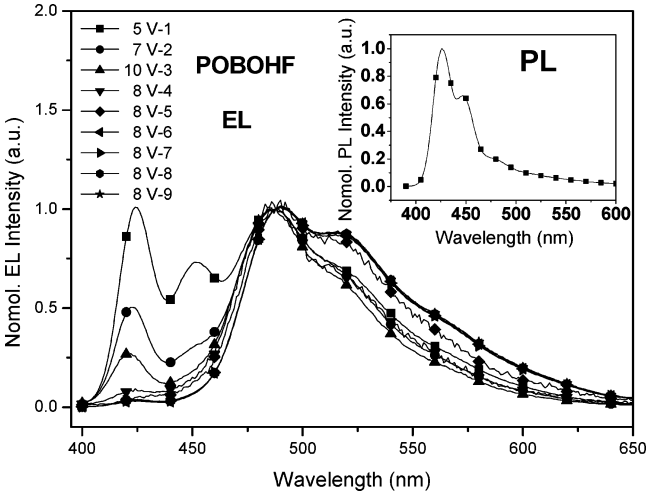

Figure 1. EL spectra measured at room temperature from POBOHF-based device (ITO/PEDOT/POBOHF/Ca/Al). Spectra were continuously collected at 5, 7, and 10 V; for the subsequent six spectra, 8 V was applied for every 20 s interval before measuring each spectrum. All the spectra were normalized at 488 nm. The inset shows the PL spectrum of POBOHF film excited at 387 nm and normalized at 426 nm.

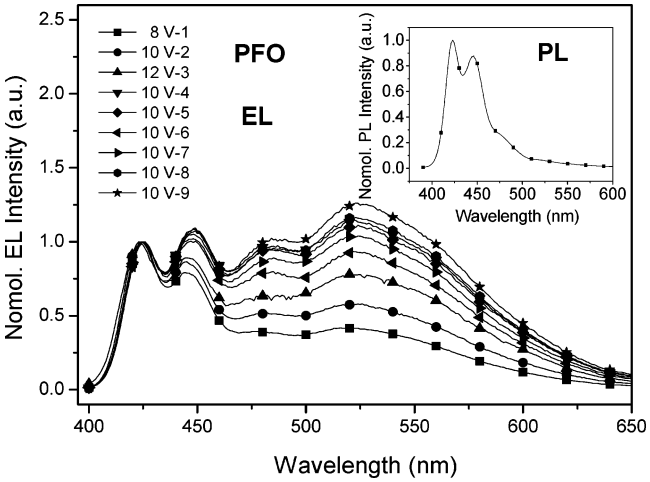

Figure 2. EL spectra measured at room temperature from PFO-based device (ITO/PEDOT/PFO/Ca/Al) and normalized at 424 nm. Spectra were continuously collected at 8, 10, and 12 V; for the subsequent six spectra, 10 V was applied for every 20 s interval before measuring each spectrum. The inset shows PL spectrum of PFO film excited at 385 nm and normalized at 423 nm.

Because the present POBOHF and PFO were end-capped with *tert*-butylphenylene, the green component should not contribute from polar end groups (i.e., bromine).[29] This does not mean that suppressing green emission by end-capping has failed. Actually, from our conjecture, end-capping can only provide effective suppression for short-term operation with PFs bearing nonpolar side chains, such as PFO. In addition, this green component should not be caused by the presence of oligomers, which have molecular weights (MW) lower than 10^4 Da as reported by Weinfurtner et al.,[30] because

Table 1. Average Molecular Weights and Polydispersity Indexes (PDIs) of PFs

	M_n	M_w	PDI
POBOHF	261 100	543 000	2.08
PFO	133 800	224 800	1.68
PF-1/1	102 900	190 400	1.57
PF-1/3	171 400	256 000	1.49

the polymers synthesized in this work are of high molecular weights (having low MW tails higher than 10^4 Da) and low polydispersity indexes (see Table 1). Since the green emission component in PFs has been extensively ascribed to the keto defect, we take PFO as an example to explore whether the keto defect is responsible for the green emission in PFs via an analysis of infrared measurements and deconvolutions of the EL spectra.

FTIR measurements were performed on PFO films before and after device fabrication (the device structure is ITO/PEDOT/PFO/Ca/Al) as well as after use (i.e., after the EL measurements as described in the caption of Figure 2). The keto defect is not found in the PFO film before deposition of Ca cathode (see the inset of Figure 3a, in which no keto characteristic peak at 1725 cm^{-1} appears), but it really occurs after deposition of calcium onto PFO film as indicated in the presence of a peak at 1725 cm^{-1} (i.e., carbonyl stretching mode), as shown in Figure 3a. From ^1H NMR spectra of monomers **3** and **4**, we can ensure that 9-monoalkylated fluorenes do not appear in these monomers, indicating that the keto defect did not form during the polymerizations of their

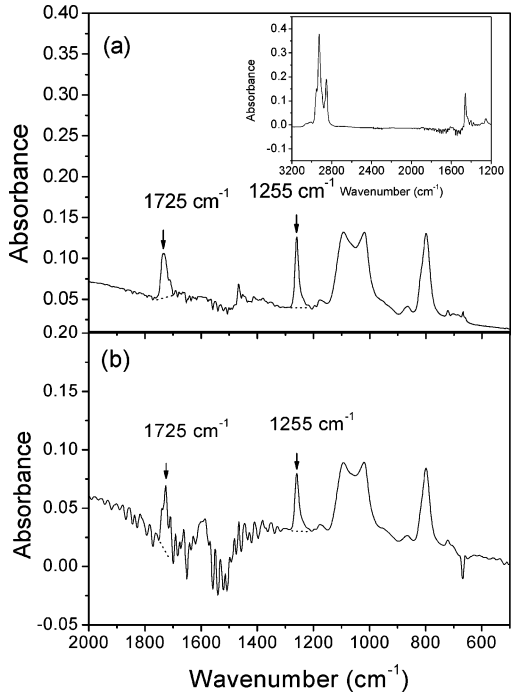

Figure 3. FTIR spectra of PFO films for (a) after device fabrication and (b) after the device was operated at 10 V for the ninth cycle. The device structure is ITO/PEDOT/PFO/Ca/Al, and the operation sequence is the same as that described in Figure 2. The films were obtained by using tapes to peel off the top metal electrodes covered on the devices. "Shot dot" lines in (a) and (b) depict the baselines used for quantitative analyses. Absorbance heights at 1255 and 1725 cm^{-1} were taken from peak maxima to the shot dot lines and used to compare the relative amounts of keto defects for devices after fabrication and after operation. The inset shows FTIR spectrum of pristine PFO film cast from its chloroform solution on KBr substrate.

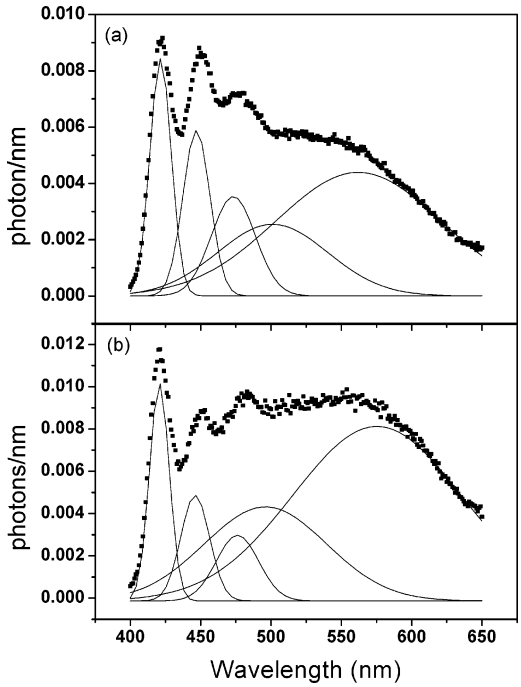

Figure 4. EL spectra measured from PFO-based device operated at (a) 8 V for the first cycle and (b) 10 V for the ninth cycle. The unit of emission intensity was converted into photons per nm for quantitative analysis purpose; that is, the areas under the peaks can represent the emitted photons. The solid lines represent the deconvolution of the spectrum into constituent components. The device structure is ITO/PEDOT/PFO/Ca/Al, and the operation sequence is the same as that described in Figure 2.

corresponding polymers (this is also supported by the FTIR data shown in the inset of Figure 3a). Since thermal annealing or exposure to UV light for the polymers was avoided during the device fabrication and operation, the keto defect cannot generate under these two conditions, and in this case, it should form during the deposition of calcium onto PFO film as was also found by Gong et al.[36] However, in addition to calcium, the keto defect might also form while using other materials as cathodes directly on top of PFs.[17,35]

We are wondering if the green emission is totally contributed from the formation of the keto defect. From Figure 3b, after the ninth cycle, the absorbance ratio of carbonyl stretching mode (located at 1725 cm^{-1}) to the C−C stretching mode between two phenylene rings belonging to adjacent monomeric units[44] (located at 1255 cm^{-1} and used as an internal standard to compensate for the variation of film thickness) is 80% larger than that just after the device fabrication. (This is direct evidence that the keto defect really occurs during the device operation.) After that, as shown in Figure 4, the EL spectra measured at 8 V for the first cycle and at 10 V for the ninth cycle (the operation sequence is the same as described in the caption of Figure 2) were deconvoluted to investigate relationship between the keto defect and green component. The deconvoluted peaks at 421 and 447 nm are assigned to the emission from isolated PFO chains,[16] and the remaining three peaks at the long-wavelength portion (at 475, 500, and 570 nm) are attributed to the emission of the keto defect.[36] It is noticeable that, for the device operated at 10 V for the ninth cycle, the ratio of the overall area of the long-wavelength component to the total spectrum is 10% larger than that operated at 8 V for the first

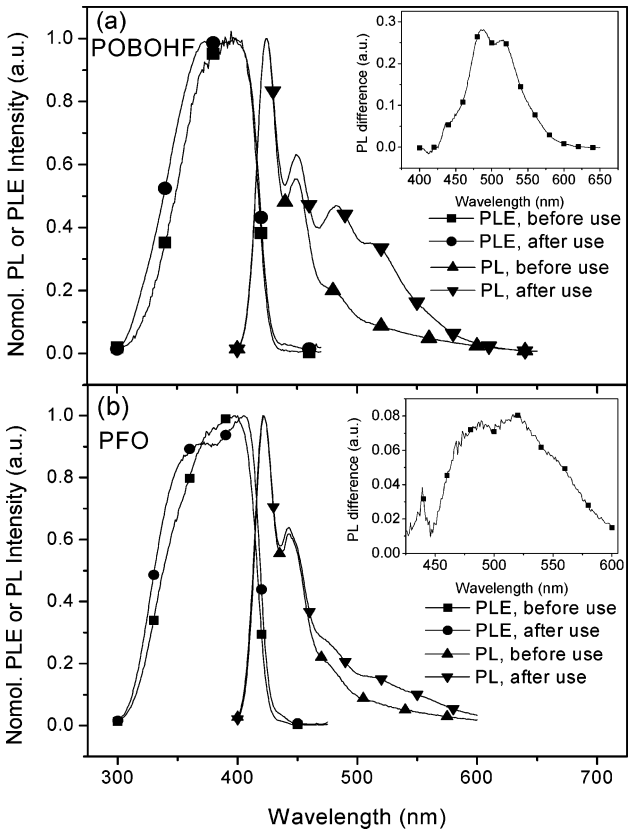

Figure 5. (a) PLE (monitored at 480 nm and normalized at 398 nm) and PL (excited at 388 nm and normalized at 423 nm) spectra measured from POBOHF-based devices before and after use. (b) PL and PLE spectra measured from PFO-based devices before as well as after use. PL spectra were excited at 388 nm and normalized at 421 nm, and PLE spectra were monitored at 480 nm and normalized at 398 and 405 nm for device before and after use, respectively. The insets in (a) and (b) show additional components formed after device operation for POBOHF and PFO, respectively, by subtracting the PL spectrum before use from that after use. All the spectra were measured by irradiating excitation light from the ITO side.

cycle. This means that the increase of the amount of the keto defect does not entirely reflect the increase in intensity of long-wavelength components. This result agrees with the observation of Bradley and co-workers in that the individual fluorenone cannot emit green emission in PL, except the close approach of polymer chains to form fluorenone-based excimers.[45] In other words, the keto defect may not be the only source for the green emission in PFs.

As a result, we compare the PL and PLE spectra of POBOHF films from devices before (that is, just after device fabrication) and after use (i.e., after the ninth cycle at 8 V as described in Figure 1) to identify origins for the green component. For the used device, the emission intensity of the long-wavelength part (470−600 nm) is obviously larger than that of the device before use (see Figure 5a). This means that excimers or aggregates are formed after the device operation. However, in the PLE spectrum, the long-wavelength tail (430−470 nm) does not increase apparently after use, indicating that excimers, but not aggregates,[46] are actually formed. In addition, from the inset of Figure 5a, the additional PL band (which is formed after the device operation and peaks at 487 nm as well as 516 nm) resembles the EL spectrum measured at the sixth to ninth cycles at 8 V in Figure 1. It is obvious that this

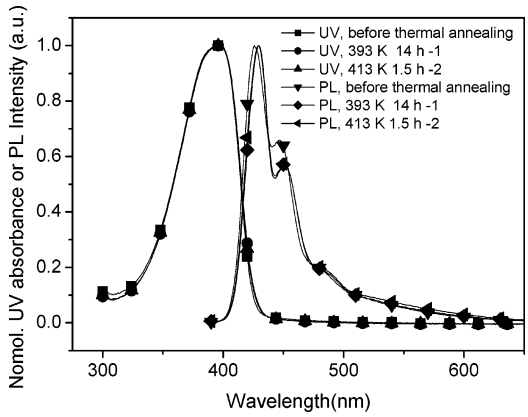

Figure 6. UV (normalized at 395 nm) and PL (excited at 387 nm) spectra of POBOHF film measured before and after thermal annealing. "1" represents the spectrum was measured after the pristine film was annealed at 393 K for 14 h. "2" represents the spectrum was measured after the same film was further annealed at 413 K for 1.5 h. The PL spectrum measured before annealing was normalized at 426 nm, and the two PL spectra measured after annealing were normalized at 429 nm.

excimer band is different from that of the fluorenone defect (featureless band with a main peak at 530 nm) as reported by Sim et al.[45] due to different shapes and positions of the main peaks in PL spectra. Hence, we attribute this excimer band to fluorene-based excimers, not fluorenone defect-based excimers.

For PFO, Figure 5b shows that the long-wavelength tail (470−600 nm) in the PL spectrum increases, but the long-wavelength part (400−475 nm) in the PLE spectrum remains almost unchanged after use. Therefore, as in the case of POBOHF, excimers also form for PFO after the device operation, and the PL excimer band is shown in the inset of Figure 5b. The intensity of the excimer emission band from PFO is apparently lower than that from POBOHF (explanation for this phenomenon will be given in section 4), but emission peaks from either PFO or POBOHF are located at 487 and 516 nm, implying they are from the same fluorene-based excimers. However, for PFO, another peak at 439 nm is more obvious than POBOHF due to the lower intentsity of the long-wavelength component (450−600 nm) for PFO.

2. Effect of Electric Field on the Formation of Excimers for POBOHF. A possible source for the generation of excimers could be the generated heat during the device operation. However, from Figure 6, none of the UV and PL spectra of POBOHF show apparent variation in intensity at the long-wavelength tails (UV: 400−475 nm; PL: 470−650 nm) after the film was thermally annealed in sequence at 393 and 413 K, which are above its glass transition temperature (T_g) (307 K measured by the FI-TSC technique as to be revealed in section 3), for 14 and 1.5 h, respectively. Therefore, the formation of excimers cannot be induced by the heat generation during the device operation.

Another possible source might be the applied electric field. We performed the EL measurements on the same POBOHF-based device at different temperatures (from 78 to 330 K) in a cryostat maintained in a vacuum less than 10^{-5} Torr. For every selected temperature, the sequence for measurements was the same as that described in the caption of Figure 1, except that 7 and 8 V, instead of 5 and 7 V, were applied for the first and second cycles, respectively. Figure 7 shows the EL

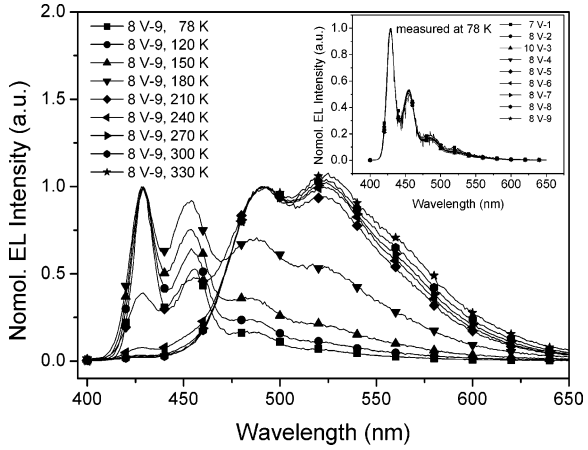

Figure 7. EL spectra measured from the same POBOHF-based device (ITO/PEDOT/POBOHF/Ca/Al) at different temperatures in a cryostat maintained at a vacuum less than 10^{-5} Torr. For every specific temperature, spectra were collected as the sequence described in Figure 1 except 7 and 8 V, instead of 5 and 7 V, were applied for the first and second cycles, respectively. Spectra measured at 8 V-9 from 78 to 180 K and 210 to 330 K were normalized at 428 and 492 nm, respectively. The inset shows EL spectra measured at 78 K as an example to express the collection sequence at every temperature (normalized at 429 nm).

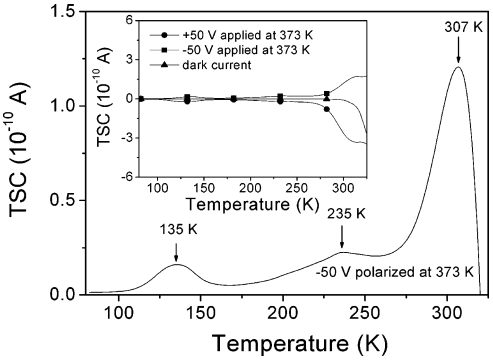

Figure 8. FI-TSC spectrum of POBOHF-based device (device structure: ITO/POBOHF/Al) after deleting absolute value of dark current from released current by polarization with −50 V at 373 K. The inset shows original plots of FI-TSC, including polarizations with +50 V as well as −50 V at 373 K and dark current from 82 to 325 K.

spectra measured at 8 V at the ninth cycle starting from 78 to 330 K, and the inset shows those measured at 78 K under 7 to 10 and then to 8 V, in which the EL spectra exhibit no appreciable change at such low temperature. The intensity of the green emission (at 520 nm) relative to that of the blue emission (at 428 nm) raises with increasing temperature, and the green component (470−650 nm) starts to dominate at about 210 K. This implies that the electric field indeed facilitates the formation of excimers, and the relaxation of side chains may also play a role in the formation of the electric-field-induced excimers (FI excimers).

3. Side-Chain-Motion-Assisted Excimers Formation for POBOHF. To investigate the relation between chain motions and FI excimers formation, FI-TSC was measured to estimate relaxation temperatures for side chain and main chain of POBOHF. Figure 8 shows the FI-TSC spectrum of POBOHF after deleting dark current from the released current, for which the device was polarized with −50 V at 373 K. As can be observed, there exist three peaks at 135, 235, and 307 K. The inset illustrates the original plots of FI-TSC measurements, including polarizations with +50 V as well as −50 V at 373 K and dark current from 82 to 325 K. The two released current profiles appear to possess same peak positions as well as symmetry in magnitude, indicating that they are contributed from depolarization rather than traps.[47] In other words, the three peaks are indicative of relaxation temperatures for side chain and main chain of POBOHF and will be assigned to specific chain motions below. For polyolefins with *n*-alkyl side chains (carbon numbers: 3−8), the side chain relaxation temperature increases from 113 to 143 K as *n* reduces from 8 to 3,[48] while for the soluble conjugated polymers, poly(3-alkylthiophene)s (P3ATs) with the carbon numbers 4, 8, and 12 of alkyl side chains, the relaxation temperatures for methylene linkages are below 123 K and those of side chains are 207 and 236 K for octyl and dodecyl side chains, respectively.[49] Therefore, we can rationally assign the peak at 135 K as the relaxation temperature for methylene linkages of *n*-alkyl side chain (six carbons) of POBOHF and designate it as the γ relaxation temperature (T_γ). In addition, Sauer et al.[50] have performed FI-TSC measurements on poly(methyl methacrylate)s (PMMAs) with different tacticities and found a side chain ($-COOCH_3$) relaxation temperature occurring from 193 to 283 K with a peak at 238 K. Besides, motion of the side chains ($-OCOCH_3$) in poly(vinyl acetate) (PVA) occurs from 230 to 293 K with a peak at 263 K.[51] Hence, according to the relaxation temperatures of side chains for P3AT, PMMA, and PVA, the peak at 235 K for POBOHF can be reasonably assigned to the relaxation temperature of the entire side chain and designated as β relaxation temperature (T_β). Moreover, since T_g of PFO main chain is at 333 K,[52] the peak at 307 K can be assigned to the relaxation temperature for the main chain of POBOHF and designated as T_α.

Here, we study the relationship between chain motions and evolution of EL spectrum. From the inset of Figure 7, it is obvious that the EL spectra at 78 K under cyclic operation (below T_γ) remain unchanged, and the green component (470−650 nm) does not grow for all the operation cycles. While the device is operated at 120 and 150 K (in the range of T_γ), the green component develops slightly, indicating that motion of methelyene leakages only slightly assists the growth of the green component. Above that temperature, the green component starts to grow significantly at 180 K, which is slightly above the onset temperature of T_β (at about 175 K). The green emission dominates the EL emission at 210 K while the blue emission peaked at 430 and 455 nm still remains; after reaching 240 K (near the peak of β relaxation), the EL spectrum contains only the green component. This implies that motion of the whole side chains dramatically affect the progression of the EL spectrum. As a result, from the evolution of EL spectra with temperature and the locations of side chain relaxation temperatures, it can be inferred that motion of side chains (especially for highly polar oxetane-containing side chains) along with the presence of electric field can align the relative orientation of two neighboring segments of main chains to form excimers, which is the origin of the green component of the emission.

4. Effect of Side-Chain Polarity on FI Excimers Formation in PFs. EL measurements at different temperatures (from 78 to 330 K) were also performed on PFO to investigate whether excimers can be induced

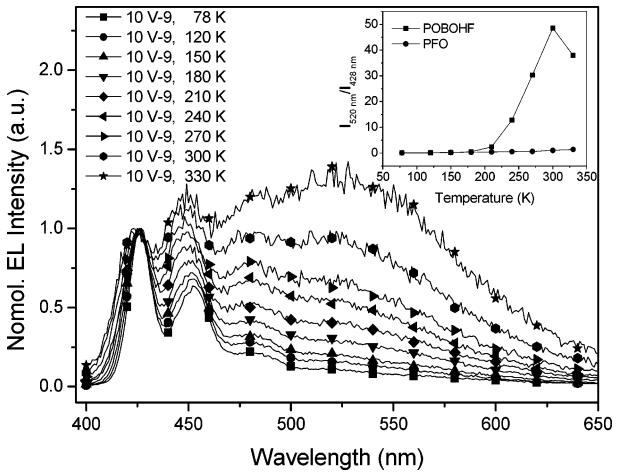

Figure 9. EL spectra from the same PFO-based device (ITO/PEDOT/PFO/Ca/Al) at different temperatures in a cryostat maintained at a vacuum less than 10^{-5} Torr. For every selected temperature, spectra were collected as the sequence described at Figure 2. All the spectra were normalized at 424 nm. The inset illustrates EL intensity ratios of 520 nm relative to 428 nm (I_{520nm}/I_{428nm}) at different temperatures for POBOHF and PFO.

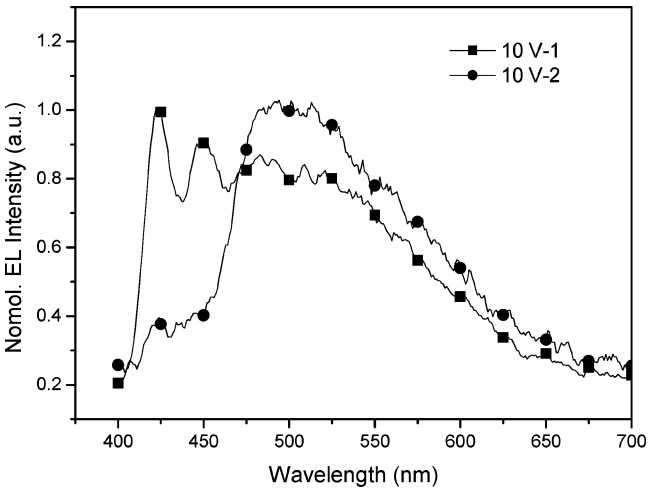

Figure 10. EL spectra measured at room temperature from cross-linked-POBOHF-based device (ITO/PEDOT/cross-linked-POBOHF/Ca/Al). The first spectrum was collected at 10 V, and the second spectrum was measured at 10 V after applying 10 V for 20 s; both were normalized at 422 and 484 nm, respectively.

by electric field with an assistance by motion of side chains. As shown in Figure 9, the green component (470−650 nm) also develops with increasing temperature under applied electric field as in the case of POBOHF. This implies that, for PFO, side chains motion under the high electric field also facilitates the formation of FI excimers.

To study effects of side chain structure in PFs on the formation of the green component in EL emission, variations of EL intensity ratio for 520 nm relative to 428 nm (I_{520nm}/I_{428nm}) with temperature for POBOHF and PFO are shown in the inset of Figure 9, which are obtained by replotting the data shown in Figures 7 and 9. It is obvious that, at 300 K, I_{520nm}/I_{428nm} for POBOHF is larger than that for PFO by about a factor of 50. Therefore, it is reasonable to deduce that motions of oxetane-containing side chains strongly induce the formation of FI excimers under an electric field due to the high polarity of oxetane groups. Although motions of side chains also help the formation of FI excimers for PFO, the extent is much lower due to the low polarity of *n*-alkyl side chains. On the other hand, we suggest that, for POBOHF, decrease of green emission at 330 K may be attributed to an interference on the FI excimers by segmental motion of the main chains because T_g of POBOHF main chain is 307 K. However, this does not happen to PFO due to its higher T_g (333 K).

5. Effect of Cross-Linking and Copolymerization on the Formation of FI Excimers. To examine whether cross-linking could suppress FI excimers, we cross-linked POBOHF and measured EL spectra at 10 V for two cycles, as shown in Figure 10. As can be seen, the green component still grows up even after the cross-linking. About copolymerization, copolymers of monomers **3** and **4** with the feed ratios by mole 1:1 and 1:3 (designated as PF-1/1 and PF-1/3, respectively) were synthesized in order to reduce a formation of FI excimers. However, as can be seen from Figure 11, these two copolymers only slightly suppress a formation of FI excimers due to the high polarity of oxetane groups in the copolymers.

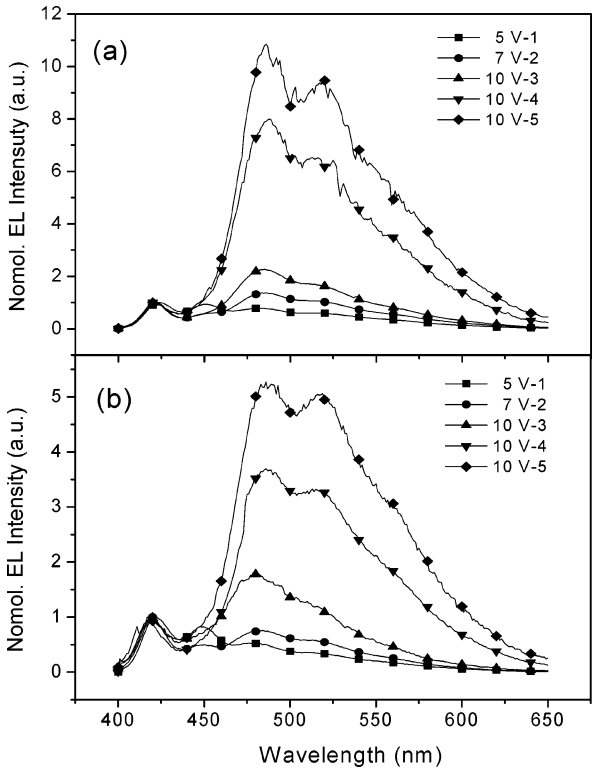

Figure 11. EL spectra measured at room temperature from devices with (a) PF-1/1 and (b) PF-1/3. The device structure is ITO/PEDOT/(PF-1/1 or PF-1/3)/Ca/Al. Spectra were continuously collected at 5, 7, and 10 V; for the subsequent two spectra, 10 V was applied for every 20 s interval before measuring each spectrum. All the spectra were normalized at 420 nm.

Conclusions

Because of the high polarity of oxetane-containing side chains, excimers in POBOHF can be strongly induced by electric field (0.8×10^6 V/cm), resulting in a dominant green emission in the EL spectrum. This phenomenon also happens to nonpolar side chain containing PFO (but to a less extent) under higher electric field (1×10^6 V/cm), the copolymer containing only 25

mol % of cross-linkable comonomer and even cross-linked POBOHF.

Acknowledgment. This work is financially supported by the Ministry of Education through project 91E-FA04-2-4A and by the National Science Council. We are also grateful for the supply of photoacid used in this work by Professor Wen-An Loong.

Supporting Information Available: Detailed experimental procedures, characterizations for all of the monomers and polymers, and instrumentation details. This material is available free of charge via the Internet at http://pubs.acs.org.

References and Notes

(1) Burroughes, J. H.; Bradley, D. D. C.; Brown, A. R.; Marks, R. N.; Mackay, K.; Friend, R. H.; Burns, P. L.; Holmes, A. B. *Nature (London)* **1990**, *347*, 539−541.
(2) Kraft, A.; Grimsdale, A. C.; Holmes, A. B. *Angew. Chem., Int. Ed.* **1998**, *37*, 402−428.
(3) Horowitz, G. *Adv. Mater.* **1998**, *10*, 365−377.
(4) Ling, M. M.; Bao, Z. N. *Chem. Mater.* **2004**, *16*, 4824−4840.
(5) Svensson, M.; Zhang, F. L.; Veenstra, S. C.; Verhees, W. J. H.; Hummelen, J. C.; Kroon, J. M.; Inganäs, O.; Andersson, M. R. *Adv. Mater.* **2003**, *15*, 988−991.
(6) Coakley, K. M.; McGehee, M. D. *Chem. Mater.* **2004**, *16*, 4533−4542.
(7) Ariu, M.; Lidzey, D. G.; Lavrentiev, M.; Bradley, D. D. C.; Jandke, M.; Strohriegl, P. *Synth. Met.* **2001**, *116*, 217−221.
(8) Bernius, M. T.; Inbasekaran, M.; O'Brien, J.; Wu, W. S. *Adv. Mater.* **2000**, *12*, 1737−1750.
(9) Neher, D. *Macromol. Rapid Commun.* **2001**, *22*, 1365−1385.
(10) Scherf, U.; List, E. J. W. *Adv. Mater.* **2002**, *14*, 477−487.
(11) Chen, X.; Liao, J. L.; Liang, Y.; Ahmed, M. O.; Tseng, H. E.; Chen, S. A. *J. Am. Chem. Soc.* **2003**, *125*, 636−637.
(12) Kreyenschmidt, M.; Klaerner, G.; Fuhrer, T.; Ashenhurst, J.; Karg, S.; Chen, W. D.; Lee, V. Y.; Scott, J. C.; Miller, R. D. *Macromolecules* **1998**, *31*, 1099−1103.
(13) Miteva, T.; Meisel, A.; Knoll, W.; Nothofer, H. G.; Scherf, U.; Müller, D. C.; Meerholz, K.; Yasuda, A.; Neher, D. *Adv. Mater.* **2001**, *13*, 565−570.
(14) Nakazawa, Y. K.; Carter, S. A.; Nothofer, H. G.; Scherf, U.; Lee, V. Y.; Miller, R. D.; Scott, J. C. *Appl. Phys. Lett.* **2002**, *80*, 3832−3834.
(15) Sainova, D.; Miteva, T.; Nothofer, H. G.; Scherf, U.; Glowacki, I.; Ulanski, J.; Fujikawa, H.; Neher, D. *Appl. Phys. Lett.* **2000**, *76*, 1810−1812.
(16) Bliznyuk, V. N.; Carter, S. A.; Scott, J. C.; Klärner, G.; Miller, R. D.; Miller, D. C. *Macromolecules* **1999**, *32*, 361−369.
(17) List, E. J. W.; Guentner, R.; Freitas, P. S. D.; Scherf, U. *Adv. Mater.* **2002**, *14*, 374−378.
(18) Lee, J. I.; Klaerner, G.; Miller, R. D. *Chem. Mater.* **1999**, *11,* 1083−1088.
(19) Gaal, M.; List, E. J. W.; Scherf, U. *Macromolecules* **2003**, *36*, 4236−4237.
(20) Gamerith, S.; Gaal, M.; Romaner, L.; Nothofer, H. G.; Güntner, R.; Freitas, P. S. D.; Scherf, U.; List, E. J. W. *Synth. Met.* **2003**, *139*, 855−858.
(21) Klärner, G.; Davey, M. H.; Chen, W. D.; Scott, J. C.; Miller, R. D. *Adv. Mater.* **1998**, *10*, 993−997.
(22) Lee, J. I.; Klaerner, G.; Miller, R. D. *Synth. Met.* **1999**, *101,* 126.
(23) Theander, M.; Johansson, D. M.; Ruseckas, A.; Zigmantas, D.; Andersson, M. R.; Sundström, V.; Inganäs, O. *Synth. Met.* **2001**, *119,* 615−616.
(24) Zeng, G.; Yu, W. L.; Chua, S. J.; Huang, W. *Macromolecules* **2002**, *35*, 6907−6914.
(25) Jenekhe, S. A.; Osaheni, J. A. *Science* **1994**, *265*, 765−768.
(26) Prieto, I.; Teetsov, J.; Fox, M. A.; Bout, D. A. V.; Bard, A. J. *J. Phys. Chem. A* **2001**, *105,* 520−523.
(27) Conwell, E. M.; Perlstein, J.; Shaik, S. *Phys. Rev. B* **1996**, *54*, 2308−2310.
(28) Chen, S. H.; Su, A. C.; Han, S. R.; Chen, S. A.; Lee, Y. Z. *Macromolecules* **2004**, *37*, 181−186.
(29) Chen, X.; Tseng, H. E.; Liao, J. L.; Chen, S. A. *J. Phys. Chem. B* **2005**, *109,* 17496−17502.
(30) Weinfurtner, K. H.; Fujikawa, H.; Tokito, S.; Taga, Y. *Appl. Phys. Lett.* **2000**, *76*, 2502−2504.
(31) Yu, W. L.; Pei, J.; Huang, W.; Heeger, A. J. *Adv. Mater.* **2000**, *12*, 828−831.
(32) Setayesh, S.; Grimsdale, A. C.; Weil, T.; Enkelmann, V.; Müllen, K.; Meghdadi, F.; List, E. J. W.; Leising, G. *J. Am. Chem. Soc.* **2001**, *123*, 946−953.
(33) Marsitzky, D.; Vestberg, R.; Blainey, P.; Tang, B. T.; Hawker, C. J.; Carter, K. R. *J. Am. Chem. Soc.* **2001**, *123*, 6965−6972.
(34) Klärner, G.; Lee, J. I.; Lee, V. Y.; Chan, E.; Chen, J. P.; Nelson, A.; Markiewicz, D.; Siemens, R.; Scott, J. C.; Miller, R. D. *Chem. Mater.* **1999**, *11*, 1800−1805.
(35) Kulkarni, A. P.; Jenekhe, S. A. *Macromolecules* **2003**, *36*, 5285−5296.
(36) Gong, X.; Iyer, P. K.; Moses, D.; Bazan, G. C.; Heeger, A. J.; Xiao, S. S. *Adv. Funct. Mater.* **2003**, *13*, 325−330.
(37) Romaner, L.; Pogantsch, A.; Freitas, P. S. D.; Scherf, U.; Gaal, M.; Zojer, E.; List, E. J. W. *Adv. Funct. Mater.* **2003**, *13*, 597−601.
(38) Yang, X. H.; Jaiser, F.; Neher, D.; Lawson, P. V.; Brédas, J. L.; Zojer, E.; Güntner, R.; Freitas, P. S. D.; Forster, M.; Scherf, U. *Adv. Funct. Mater.* **2004**, *14*, 1097−1104.
(39) Kulkarni, A. P.; Kong, X.; Jenekhe, S. A. *J. Phys. Chem. B* **2004**, *108*, 8689−8701.
(40) Craig, M. R.; Kok, M. M. D.; Hofstraat, J. W.; Schenning, A. P. H. J.; Meijer, E. W. *J. Mater. Chem.* **2003**, *13*, 2861−2862.
(41) Gamerith, S.; Nothofer, H. G.; Scherf, U.; List, E. J. W. *Jpn. J. Appl. Phys.* **2004**, *43*, 891−893.
(42) Teetsov, J.; Bout, D. A. V. *Langmuir* **2002**, *18*, 897−903.
(43) Yang, Y.; Pei, Q. B. *J. Appl. Phys.* **1997**, *81*, 3294−3298.
(44) Ariu, M.; Lidzey, D. G.; Bradley, D. D. C. *Synth. Met.* **2000**, *111−102*, 607−610.
(45) Sims, M.; Bradley, D. D. C.; Ariu, M.; Koeberg, M.; Asimakis, A.; Grell, M.; Lidzey, D. G. *Adv. Funct. Mater.* **2004**, *14*, 765−781.
(46) Peng, K. Y.; Chen, S. A.; Fann, W. S. *J. Am. Chem. Soc.* **2001**, *123*, 11388−11397.
(47) Bräunlich, P.; Dewerd, L. A.; Fillard, J. P.; Gasiot, J.; Glaefeke, H.; Kelly, P.; Lang, D. V.; Vanderschueren, J. *Thermally Stimulated Relaxation in Solids*; Springer-Verlag: Berlin, 1979.
(48) McCrum, N. G.; Read, B. E.; Williams, G. *Anelastic and Dielectric Effects in Polymeric Solids*; Dover: New York, 1991; pp 387−389.
(49) Chen, S. A.; Ni, J. M. *Macromolecules* **1992**, *25*, 6081−6089.
(50) Sauer, B. B.; Kim, Y. H. *Macromolecules* **1997**, *30*, 3323−3328.
(51) McCrum, N. G.; Read, B. E.; Williams, G. *Anelastic and Dielectric Effects in Polymeric Solids*; Dover: New York, 1991; pp 313−317.
(52) Grell, M.; Bradley, D. D. C.; Inbasekaran, M.; Woo, E. P. *Adv. Mater.* **1997**, *9*, 798−802.

MA051594Z